

Effect of Cyclone Thane in the Bay of Bengal Explored Using Moored Buoy Observations and Multi-platform Satellite Data

Neethu Chacko¹  · Leimiwon Zimik²

Received: 5 October 2017 / Accepted: 28 December 2017 / Published online: 8 March 2018
© Indian Society of Remote Sensing 2018

Abstract

This work examines the response of the upper ocean during the passage of cyclone Thane (December 25–30, 2011) over the Bay of Bengal. Observations from a moored buoy are employed to assess the changes in the upper 100 m depth of the ocean. Observations revealed strong temperature inversion prevailing in this region. The temperature inversion resulted in varying response in the subsurface, with warming in the upper 40 m depth and cooling in the depths of 40–80 m at the moored buoy location. Analysis of subsurface temperature and salinity revealed the signatures of vertical mixing induced by Thane. The subsurface currents are observed as strongly responding to the cyclone winds. Analysis revealed that the influence of Thane was generally confined to within 100 m depth. Intense biological response is revealed along the track of the cyclone. However, the bloom is localized in two distinct regions: one in the central Bay and other off the south-western coastal region. This is attributed to the intense Ekman pumping velocity, slow translation speed and the availability of nitrate concentration in the shallow coastal waters.

Keywords Thane · Cyclone · Chlorophyll blooms · Temperature inversion · Bay of Bengal

Introduction

Tropical cyclones are extreme events which cause strong changes in the upper ocean. Though transient in nature, tropical cyclones cause re-distribution of heat and salt locally. Various observational and modeling studies indicate that tropical cyclones cause strong vertical mixing and upwelling which brings cooler deep waters to the ocean surface (Price 1981). Cooling of sea surface temperature (SST) is a major change which occurs after the passage of a cyclone. The cooling of SST is primarily caused by vertical mixing induced entrainment of cooler waters from below the mixed layer and transient upwelling (Price 1981; Dickey et al. 1998). The enhanced sensible and latent heat

fluxes from the ocean to the atmosphere driven primarily by the high cyclone winds also contribute to SST cooling. Another remarkable phenomenon induced by cyclones is the enhancement of biological productivity in the ocean (Subrahmanyam et al. 2002; Lin et al. 2003; Shang et al. 2008). In addition to these changes, tropical cyclones impact various oceanic parameters like mixed layer depth, salinity (Maneesha et al. 2012; Domingues et al. 2015) and ocean currents (Venkatesan et al. 2014).

Though various studies have reported on the physical and biological responses induced by cyclones in all the oceanic basins, most of these studies are based on surface observations. It is also widely noted that cyclones induced changes are highly dependent on the inter-play between the cyclone characteristics and the pre-cyclone oceanic conditions (Dickey et al. 1998). Sengupta et al. (2008) showed that due to the presence of barrier layers, even the strongest cyclones could induce less SST cooling in the northern Bay of Bengal during post-monsoon season. The role of pre-existing barrier layers in inhibiting cyclone induced cooling in the surface and subsurface layers is also well documented (Wang et al. 2011; Vissa et al. 2013; Balaguru et al. 2012). Lin (2012) observed that the most intense Category 5 cyclone Maemi (2003) could not induce

Electronic supplementary material The online version of this article (<https://doi.org/10.1007/s12524-017-0748-9>) contains supplementary material, which is available to authorized users.

✉ Neethu Chacko
neethuchacko@gmail.com

¹ Regional Remote Sensing Centre-East/NRSC, ISRO, BG2, AAIB, Newtown, Kolkata 6700156, India

² Earth Science Department, Indian Institute of Technology, Bhubaneswar, Odisha, India

chlorophyll bloom in the western north Pacific. The low biological productivity is attributed to the presence of warm core features along its path and faster translation speed of Maemi. A similar observation is documented by Shi and Wang (2008) on the absence of chlorophyll bloom by Super cyclone Nargis (2008) in the Bay of Bengal. These studies indicate that ocean response to cyclones varies under different oceanic conditions and cyclone characteristics. In this perspective, we document the significant responses of ocean physical and biological properties due to cyclone Thane using satellite data and observations from a moored buoy located near to the track of the cyclone. Our emphasis is on the subsurface changes induced by Thane on physical parameters temperature, salinity and ocean currents in the upper 100 m depth. We also present the explanation for the distinctly localized chlorophyll bloom patches observed after the passage of Thane. The results presented here help improve the understanding of the subsurface response to cyclone forcing.

Data and Methods

Cyclone Thane was the strongest tropical cyclone of 2011 within the north Indian Ocean, falling under the category 2 of Saffir–Simpson scale. Thane made land fall on December 30 on the north Tamil Nadu coast. The cyclone track data is obtained from India Meteorological Department. The dataset contains time series of the cyclone center positions and wind speeds at 6-hourly intervals. The following satellite products are used in the present study. The microwave daily SST with spatial resolution of 0.25×0.25 degrees is obtained from Tropical Rain Measuring Mission (TRMM) Microwave Imager (TMI). The microwave data products can overcome the influence of cloudy conditions during cyclones. Therefore, this product can provide continuous SST observations with a better resolution during cyclone activity. Daily wind speed data from ASCAT satellite with a spatial resolution of 0.25×0.25 degrees is obtained from las.incois.gov.in (Devender et al. 2013). Chlorophyll-*a* concentration data with 4 km spatial resolution is obtained from MODIS-Aqua, produced and distributed by NASA Ocean Color. Due to high cloud coverage in this period, 8-day composite images of chlorophyll-*a* concentration are used to evaluate the biological activity following cyclone Thane. Subsurface observations from a moored buoy which is deployed by Ocean Observation Network (OON) programme of ESSO MoES of National Institute of Ocean Technology is employed in this study. These buoys deployed in the Bay of Bengal and Arabian Sea offers area the most suitable and dependable platforms for uninterrupted data collection at

fixed locations during all weather conditions throughout the year. The high temporal resolution of the mooring data (daily) is sufficient enough to capture the temporal evolution of the ocean response to the cyclone. The surface winds, subsurface observations of temperature, salinity and current speed and direction from the moored buoy BD11 used in the study is provided by Indian National Centre for Ocean Information Services. The moored buoy (BD11) is located at 83.15°E and 13.5°N . Cyclone Thane passed near the buoy location on December 28. Due to unavailability of in situ nitrate observations, climatological vertical profile of nitrates obtained from World Ocean Atlas 2013 (WOA13) is used as a proxy to show the distribution of nutrients. Turbulent air–sea fluxes (latent and sensible heat fluxes) are analyzed using Objectively Analyzed air–sea fluxes (OAFlux) daily products of 1×1 degree resolution.

Mixed Layer Depth is computed following (Rao and Sivakumar 2003). Ekman pumping velocity is an important index for assessing the upwelling in the ocean and is estimated using the ASCAT derived winds using the equations,

$$\text{WindStress}, \tau = \rho_{\text{air}} C_d U^2$$

$$\text{Ekman pumping velocity} = \text{Curl}(\tau) / \rho_w \times f$$

where, ρ_{air} is the density of air (1.25 kg/m^3), C_d is wind-drag coefficient (1.3×10^{-3}) which is a dimensionless quantity, U is the wind speed, ρ_w is the density of seawater (1025 kg/m^3) and f is the Coriolis parameter. The translation speed of Thane is derived following Mei et al. (2012).

Upper Ocean Response to Thane

Before Thane, wind field in the Bay of Bengal is characterized by lower speeds ($< 7 \text{ m/s}$) (Fig. 1a). With the arrival of Thane, winds become stronger reaching a maximum value of 14 m/s (Fig. 1b). The wind vectors overlaid on the wind speed map clearly shows the cyclonic wind distribution of Thane. Rain rate observations revealed increase in rainfall from ~ 0 to $\sim 4 \text{ mm/h}$ during Thane in the southern Bay of Bengal (figure not shown). Exchange fluxes at the air–sea interface, especially the latent and sensible heat fluxes, are important factors for the generation and maintenance of cyclones. The variations of latent and sensible heat fluxes during Thane are shown in Fig S1. During the initial stages of Thane (December 26) latent heat flux in the southwestern Bay of Bengal is $\sim 180 \text{ W/m}^2$. Usually, the latent heat flux increases during the intensification stages of cyclones (Krishna and Rao 2009; Vissa et al. 2012). With the intensification of Thane, it is observed that latent heat flux increases in the oceanic region adjacent to the cyclone track. The latent heat flux

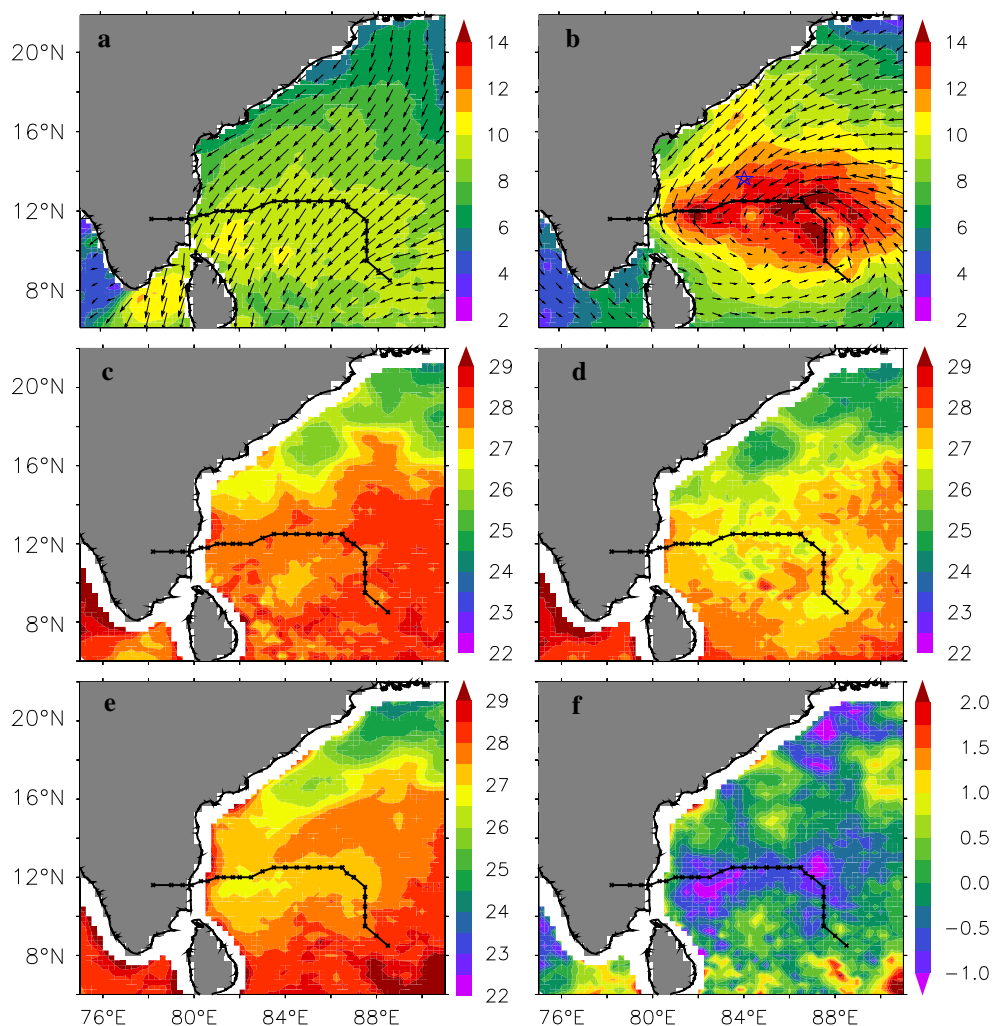


Fig. 1 ASCAT derived wind speed and wind vectors **a** before Thane (18–24 December) and **b** during Thane (25–30 December). The Star in the figure denote the position of the moored buoy BD11. TMI SST averaged for **c** 1 week before (18–24 December), **d** during Thane

(25–30 December) and **e** week after Thane (31 December–07 January). Track of the cyclone Thane is overlaid in all panels. TMI SST difference map. **f** depicting post-Thane (31 December–07 January) minus pre-Thane (18–24 December)

values are $200\text{--}220\text{ W/m}^2$ over the regions east of 84°E where Thane attained very severe cyclone status. Latent heat flux reduces to $< 100\text{ W/m}^2$ once Thane makes landfall which implies a strong dependence of wind speed to the latent heat flux. Similarly, sensible heat fluxes also increases with the increase in cyclone intensity reaching its maximum $\sim 40\text{ W/m}^2$. After Thane makes landfall, the sensible heat fluxes reduces sharply. Sensible heat flux depends on air–sea temperature difference and wind (Perrie et al. 2004). Reduction of wind and SST cooling (described in “SST Response” section) due to the cyclone resulted in the reduction of sensible heat flux.

SST Response

The evolution of SST before, during and after the period of Thane is shown in Fig. 1c–e. Before the cyclone it can be

observed that regions south of 18°N latitude is warm ($\sim 27.5\text{--}29^\circ\text{C}$, Fig. 1c) compared to northern Bay of Bengal. During Thane, it is observed that the SST in the southern Bay of Bengal dropped to $\sim 26^\circ\text{C}$ especially in the regions near to the cyclone track (Fig. 1d). Post-cyclone SST shown in Fig. 1e shows values of $\sim 27\text{--}28^\circ\text{C}$ which depicts the tendency of the ocean to restore the SST to the pre-storm values. The difference between the SSTs before and after the cyclone (Fig. 1f) shows that the sea surface cooled up to $\sim 1\text{--}1.5^\circ\text{C}$ in response to Thane. A well marked cooling can be seen along the track. Slight leftward bias of SST cooling can be seen in the regions near to the coast in contrast to the well established reports of rightward bias to the track of cyclones (Price 1981). A similar scenario of leftward bias of SST cooling is reported in the coastal regions after the super cyclone of year 1999 in Bay of Bengal (Mahapatra et al. 2007). Using numerical

simulations they claimed that while cyclones passes over coastal regions, the coastal dynamics shifts the region of maximum surface cooling towards the left of the cyclone track.

Response of Subsurface Temperature and Salinity

It is reported by many researchers that the responses of the ocean to cyclones are not limited to surface alone. Vertical structure of both physical and biological parameters responds to strong forcing events like cyclones (Girishkumar et al. 2014; Domingues et al. 2015; Chacko 2017). Response of the upper ocean is analyzed using observations from a Moored buoy which was located ~ 100 km right to the track of Thane. The temporal evolution of the subsurface temperature from 5 to 100 m depth is shown in Fig. 2a. Interestingly, the time series of the vertical thermal structure indicates the thermal inversion prevailing in this region. Thermal inversion in the Bay of Bengal, a warm layer sandwiched between surface and subsurface cooler

layers during winter is been reported by many studies (Thadathil et al. 2002; Jian et al. 2012; Girishkumar et al. 2013). Due to the large amount of freshwater input into the bay, the near-surface layer exhibits salinity-induced stratification, which is beneficial to the formation of temperature inversions. Before Thane, the water column in the upper 30 m depth shows temperature values ranging 26–27 °C above the temperature inversion layer where temperatures are up to 29–30 °C. Before the passage of cyclone the mixed layer depth is approximately 30 m. But with the arrival of cyclone, it can be seen that the mixed layer deepens from 30 to 55 m depth. Figure S2 shows the evolution of mixed layer depth and isothermal layer during Thane. A thick barrier layer (the layer between the isothermal layer depth and mixed layer depth) ~ 60 m is prevalent at this location prior to the passage of Thane. With the passage of Thane at this location, the mixed layer deepens and the isothermal layer shoals resulting in thinning the barrier layer. During Thane, the barrier layer thickness is observed to be reduced to ~ 25 m. As the barrier layer thickness reduces, exchange between

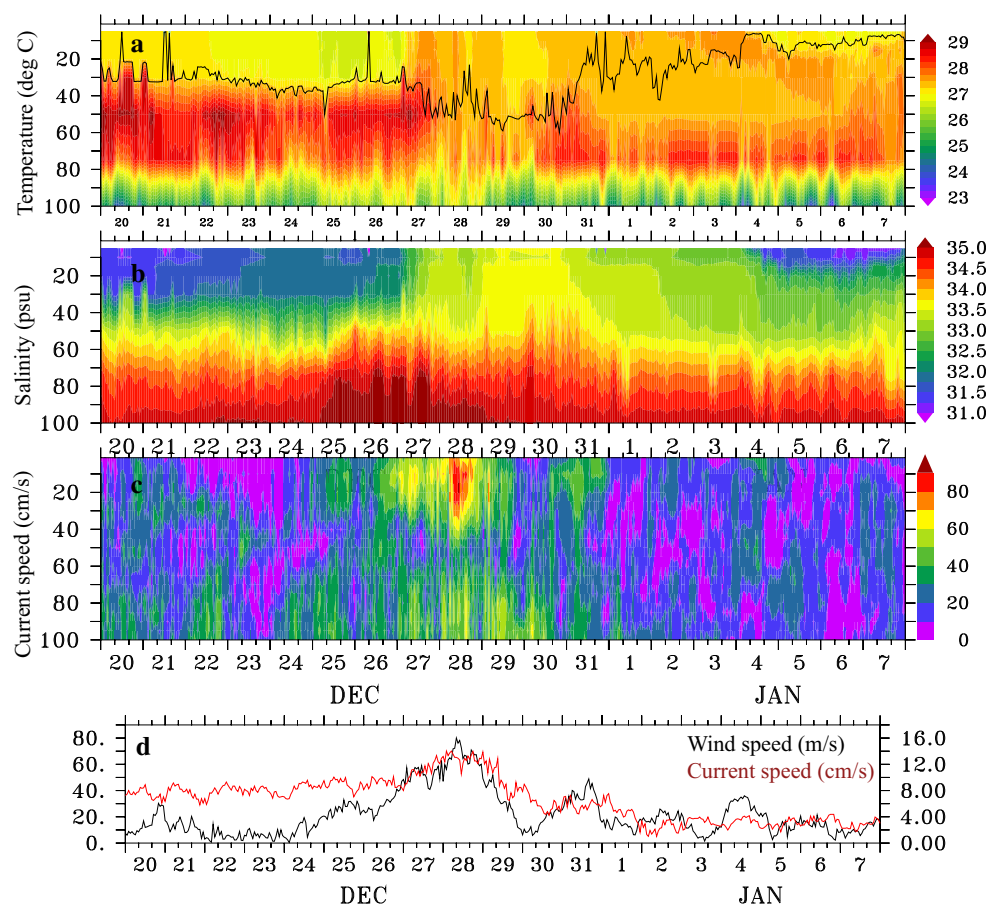


Fig. 2 Observations from the moored buoy BD11 showing the time series distribution of subsurface **a** temperature and **b** salinity and **c** current speed up to 100 m depth during Thane. **d** Shows the time

evolution of surface wind speed and current speed at surface (1.2 m) recorded by the moored buoy BD11

subsurface and mixed layer is facilitated. Vertical mixing induced outcropping of isothermals is visible from below 40 m depth towards the surface. Interestingly, before Thane the temperature at the near surface (5 m) was $\sim 26^\circ\text{C}$ and after the Thane the temperature increased to $\sim 28^\circ\text{C}$. In a normal scenario, vertical mixing induced by the cyclones results in the upwelling of cooler subsurface water which subsequently cools the upper ocean. However, temperature inversion present at this location has resulted in a net increase in the temperature values in the upper layer of the ocean. De Boyer Montégut et al. (2007) has reported on the impact of subsurface temperature inversion in affecting the entrainment of warmer subsurface temperature into the mixed layer which results in warming of SST. The thick temperature inversion layer present at this location resulted in differential vertical response: with warming in the upper 40 m depth and cooling in the 50–80 m depth. The upswing of isotherms can be observed up to 80 m depth. In the upper 20 m depth, 5 days after Thane, the temperature values are recovered closer to the pre-Thane values. Below this, up to ~ 40 m depth, the temperature values are not recovered in this period. The recovery time in the near surface and subsurface ocean can vary from a few days to few weeks (Mrvaljevic et al. 2013). Similarly, response of the subsurface salinity structure to Thane is assessed using salinity measurements from the moored buoy. Figure 2b shows the subsurface salinity up to 100 m depth during the cyclonic period. It can be observed that before Thane, the upper ocean salinity (0–30 m) is low (< 32 psu). Vertical mixing induced by the Thane results in significant increase in the salinity (~ 33.5 psu) in the upper 40 m depth. The upper ocean salinity (< 20 m) gets restored 5 days after the cyclone.

Ocean Currents

During cyclone events, a very large amount of potential and kinetic energy is injected into the ocean surface layer from the strong cyclone winds. The moored buoy measurements recorded increase in the subsurface current speed due to the cyclone winds. Figure 2c shows the evolution of subsurface currents observed by the moored buoy BD11. Sudden increase in the current speed is observed with the passage of Thane reaching maximum value of ~ 90 cm/s on December, 28. The current speed decreases from then onwards and the pre-cyclone conditions are restored soon after the passage of the cyclone by January 1. Figure 2d shows the observed current speed at 1.2 m depth along with surface wind speed measured by the moored buoy. The surface winds increases from 7 to 12 m/s during Thane. In response to the increasing wind speed, it can be observed that the current speed increases from 20 to 80 m/s, the maximum value observed on

December, 28. After this peak the current speed decreases and is restored to the pre-cyclone values. The observations thus reveals that the upper ocean currents strongly respond to the cyclone wind forcing.

Biological Response

The surface chlorophyll-*a* in the BOB displayed great spatial variation in response to Thane. Chlorophyll-*a* images obtained from MODIS-aqua data shows the distribution of surface chlorophyll-*a* concentration in the Bay of Bengal post-Thane (Fig. 3a). Large scale chlorophyll-*a* concentration enhancement is observed along the track of Thane. However, the chlorophyll bloom is localized in two distinct regions: one in the central Bay and other off the south-western coastal region of India. These two regions are denoted by two Boxes: Box1 ($80.5\text{--}83^\circ\text{E}$, $9.5\text{--}13^\circ\text{N}$) and Box2 ($85.5\text{--}88^\circ\text{E}$, $10.75\text{--}14^\circ\text{N}$). It can also be noted that the concentration of chlorophyll-*a* in the Box1 is higher than in Box2. Widely spread patches of high chlorophyll-*a* up to 2.5 mg/m^3 can be observed in the Box1. Time series of chlorophyll-*a* concentration averaged for the two boxes (Fig. 3b) shows that prior to Thane both regions are having lower chlorophyll-*a* concentrations $\sim 0.2\text{ mg/m}^3$. During the passage of Thane, the chlorophyll-*a* concentration increases significantly from 0.2 mg/m^3 to 1.3 and 0.9 mg/m^3 in Box1 and Box2 respectively on December 30. After Thane, the concentration of chlorophyll-*a* starts decreasing, and it reaches the pre-cyclone

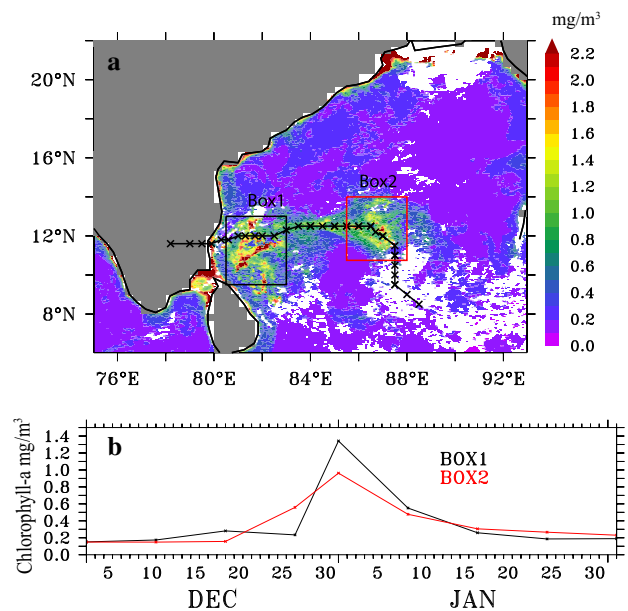


Fig. 3 a Chlorophyll-*a* image obtained from MODIS-aqua showing blooms in two distinct areas (Box1 and Box2) induced by Thane. b Concentration of chlorophyll-*a* averaged in Box1 (black) and Box2 (red) (color figure online)

values by January 15. The cyclone induced chlorophyll bloom exists for 2 weeks after the cyclone.

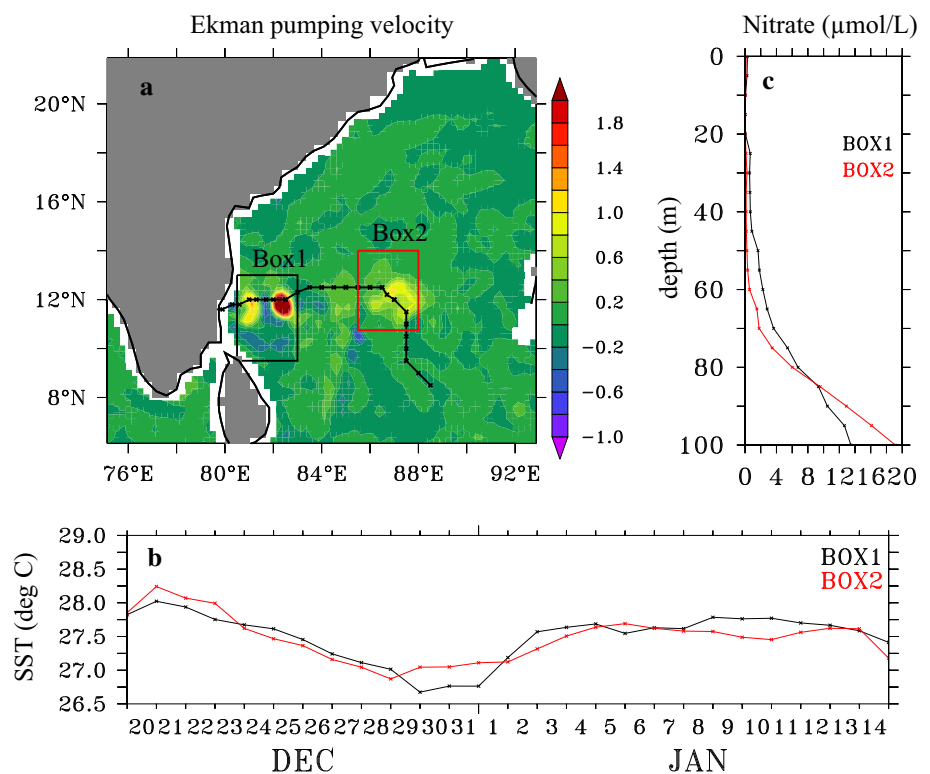
Cyclone induced chlorophyll production in the ocean surface depends on several factors. Upwelling is the physical process which brings cold subsurface water from below the thermocline. Upwelling enriches the upper euphotic zone with chlorophyll and nutrients from the subsurface and can produce phytoplankton blooms (Babin et al. 2004; Lin et al. 2003; Walker et al. 2005). Wind induced Ekman pumping velocity is an index for upwelling in the ocean with positive (negative) values indicating upwelling (downwelling). Ekman pumping velocity computed from ASCAT winds are shown in Fig. 4a. The areas of stronger upwelling coincide with the areas of high chlorophyll-*a* concentration. The cold waters upwelled from the subsurface into the upper mixed layer results in cooling of the SST. The SST response to a passing cyclone is an indication of the upwelling. SST from TMI averaged for the two boxes are shown in Fig. 4b. It can be observed that after cyclone, SST cooling observed in Box1 is more prominent (~ 0.5 °C) than in Box2. This substantiates the intense upwelling prevailed in Box1 than compared to Box2.

Another factor which influences the response of the upper ocean to tropical cyclone forcing is the translation speed of the cyclone. A slower translation speed results in longer lingering time for the cyclone over a region and can exert much longer influence on the upper ocean. Slow

moving of the cyclones can enhance the tendency of entrainment mixing and upwelling, which induces more injection of subsurface chlorophyll and nutrients into the surface waters. Studies by Sun et al. (2010), Lin (2012) and Mei et al. (2015) attributed the strong phytoplankton bloom to slower translation speed and longer transit time. The average translation speeds of Thane in Box1 and Box2 are estimated as 1.99 and 2.29 m/s respectively. The slower translation speed of the cyclone in Box1 exerted longer forcing time to establish strong upwelling in this region compared to Box2. As a result, the mixing was enhanced (entrainment and upwelling) which leads to the stronger blooms in that area.

Increase in surface chlorophyll-*a* concentration can be primarily attributed to vertical advection of chlorophyll-*a* and entrainment of nutrients from below which results in new production of chlorophyll. Hence availability of subsurface chlorophyll-*a* and nutrients play major role in determining the chlorophyll bloom induced by cyclones. Due to non-availability of subsurface chlorophyll data in this period, contribution due to chlorophyll could not be quantified. In this analysis, distribution of nitrates is used as a proxy for the nutrients in the upper ocean during the passage of Thane due to unavailability of the other nutrients data. Figure 4c shows the vertical nitrate concentration averaged for the boxes for the month of January. The nitrate concentration in both the regions is near zero in the upper 30 m depth. But the nitrate concentration in the

Fig. 4 **a** Ekman pumping velocity (m/s) averaged during the period of Thane (25–30 December). **b** Temporal evolution of TMI SST averaged for the two boxes. Black and red lines denote SST corresponding to Box1 and Box2 respectively. **c** Vertical distribution climatological nitrate ($\mu\text{Mol L}^{-1}$) averaged in the two boxes (color figure online)



Box1 increases substantially from 20 m depth, whereas in Box2, the nitrate concentration remains near zero up to 50 m depth. Compared to the two regions, Box1 is enriched with nitrates in the upper 80 m of depth. This could be due to proximity of the coast where runoff from the land contributes to strong nutrient concentration. Wind induced intense upwelling in the Box1 brings nitrate rich subsurface waters towards the surface easier. The increased supply of nitrates into the upper layer of the ocean results in new production and pronounced chlorophyll bloom.

Conclusions

In this study, we used multi-platform satellites and in situ observations to examine the upper ocean response to cyclone Thane in the Bay of Bengal. Satellite derived SST, winds, chlorophyll-*a* concentration and in situ observations of subsurface temperature, salinity and currents provided insights into the biophysical response of the upper ocean to the cyclone Thane. The effect of cyclone Thane in the upper ocean is summarized in Table 1. Significant SST cooling is detected along the track of the cyclone, with maximum cooling of 1–1.5 °C. The vertical mixing induced by the winds of the cyclone is evident in the vertical distribution of temperature and salinity recorded by a moored buoy. Results indicated varying response with increase in temperature above 40 m and decrease in temperature in 40–80 m depth. Warming of the upper ocean due to Thane is indeed due to the thermal inversion prevailing in the region. Subsurface salinity is observed as increasing in the upper 60 m depth due to the vertical mixing induced by the cyclone. Enhancement of subsurface currents is observed in response to Thane with maximum currents occurring in the upper 40 m depth. Subsurface observations revealed that the influence of Thane was generally confined to within 100 m depth. High concentration of surface chlorophyll-*a* is induced by the Thane

with the blooms localized in two distinct regions one in the central Bay and other off the south-western coastal region. Estimations of Ekman pumping velocity suggested that the region off the coastal region exhibited higher upwelling. The slower translation speed of Thane over this region also accounted for the enhanced vertical mixing of subsurface nutrients and chlorophyll-*a* into the surface layers. The higher nitrate concentration in the shallow waters also favored in generating strong bloom in south-western coastal region.

Acknowledgements Leimiwon Zimik thank Dr. Debadatta Swain, Assistant Professor, School of Earth, Ocean and LCimate Sciences, IIT Bhubaneswar for his support in carrying out this work. Moored buoy data is provided from Indian National Centre for Ocean Information Services (INCOIS). We thank Ocean Observation Programme of the National Institute of Technology (NIOT), Chennai, for the deployment and maintenance of the moored buoy. The TMI SST is downloaded from Live Access Server (LAS) of Indian National Centre for Ocean Information Services (INCOIS) (las.incois.gov.in). We acknowledge WHOI OAFflux project for providing valuable air-sea latent heat flux data. All the figures are plotted using Ferret. Authors thank two anonymous reviewers whose suggestions helped in improving the manuscript.

References

- Babin, S. M., Carton, J. A., Dickey, T. D., & Wiggert, J. D. (2004). Satellite evidence of hurricane-induced phytoplankton blooms in an oceanic desert. *Journal Geophysical Research*, *109*, C03043. <https://doi.org/10.1029/2003JC001938>.
- Balaguru, K., Chang, P., Saravanan, R., Leung, R. L., Xu, Z., Li, M., Hsieh, J. S. (2012). Ocean barrier layers's effect on tropical cyclone intensification. *Proceedings of National Academy of Sciences*, *109*, 14343–14347. <https://doi.org/10.1073/pnas.1201364109>.
- Chacko, N. (2017). Chlorophyll bloom in response to tropical cyclone Hudhud in the Bay of Bengal: Bio-argo subsurface observations. *Deep Sea Research Part I: Oceanographic Research Papers*, *112(4)*, 66–72. <https://doi.org/10.1016/j.dsr.2017.04.010>.
- De Boyer Montégut, C., Vialard, J., Shenoi, S. S. C., Shankar, D., Durand, F., Etheé, C., Madec, G. (2007). Simulated seasonal and interannual variability of the mixed layer heat budget in the northern Indian Ocean. *Journal of Climate*, *20*, 3249–3268. <https://doi.org/10.1175/JCLI4148.1>.
- Devender, R., Udaya Bhaskar, T. V. S., & Rao, E. P. R. (2013). INCOIS live access server: A platform for serving the geospatial data of Indian Ocean. *International Journal of Oceans and Oceanography*, *7(2)*, 143–151.
- Dickey, T., Frye, D., McNeil, J., Manov, D., Nelson, N., Sigurdson, D., Jannasch, H., Siegel, D., Michaels, T., Johnson, R. (1998). Upper-ocean temperature response to Hurricane Felix as measured by the Bermuda Testbed Mooring. *Monthly Weather Review*, *126*, 1195–1201. [https://doi.org/10.1175/1520-0493\(1998\)126<1195:UOTRTH>2.0.CO;2](https://doi.org/10.1175/1520-0493(1998)126<1195:UOTRTH>2.0.CO;2).
- Domingues, R., Goni, G., Bringas, F., Lee, S. K., Kim, H.-S., Halliwell, G., Dong, J., Morell, J., Pomaes, L. (2015). Upper ocean response to Hurricane Gonzalo (2014): Salinity effects revealed by targeted and sustained underwater glider observations. *Geophysical Research Letters*, *42*, 7131–7138. <https://doi.org/10.1002/2015GL065378>.

Table 1 Changes of various parameters in response to cyclone Thane

Parameter	Pre-cyclone	Post-cyclone
Winds	7 m/s	14 m/s
Rainfall	0 mm/h	4 mm/h
SST	28 °C	27 °C
Mixed layer depth	30 m	55 m
Subsurface temperature	26 °C	28 °C
Subsurface salinity	32 psu	33.5 psu
Currents at 1.2 m	20 cm/s	80 cm/s
Chlorophyll- <i>a</i> concentration	0.2 mg/m ³	2.2 mg/m ³

- Girishkumar, M. S., Ravichandran, M., & McPhaden, M. J. (2013). Temperature inversions and the influence on the mixed layer heat budget during the winters of 2006–2007 and 2007–2008 in the Bay of Bengal. *Journal of Geophysical Research: Oceans*, 118, 2426–2437. <https://doi.org/10.1002/jgrc.20192>.
- Girishkumar, M. S., Suprit, K., Chiranjivi, J., Udayabhaskar, T. V. S., Ravichandran, M., Venkat Shesu, R., Rao, E. P. R. (2014). Observed oceanic response to tropical cyclone Jal from a moored buoy in the south-western Bay of Bengal. *Ocean Dynamics*. <https://doi.org/10.1007/s10236-014-0689-6>.
- Jian, L., Lei, Y., Qiang, S. Y., & Xiao, W. D. (2012). Temperature inversion in the Bay of Bengal Prior to the summer monsoon onsets in 2010 and 2011. *Atmospheric and Oceanic Science Letters*, 5(4), 290–294. <https://doi.org/10.1080/16742834.2012.11447004>.
- Krishna, K. M., & Rao, S. R. (2009). Study of the intensity of super cyclonic storm GONU using satellite observations. *International Journal of Applied Earth Observation and Geoinformation*, 11, 108–113.
- Lin, I. I. (2012). Typhoon-induced phytoplankton blooms and primary productivity increase in the western North Pacific subtropical ocean. *Journal Geophysical Research*, 117, C03039. <https://doi.org/10.1029/2011JC007626>.
- Lin, I., Liu, W. T., Wu, C. C., Wong, G. T. F., Hu, C., Chen, Z., Liang, W. D., Yang, Y., Liu, K. K. (2003). New evidence for enhanced ocean primary production triggered by tropical cyclone. *Geophysical Research Letters*, 30(13), 1718. <https://doi.org/10.1029/2003GL017141>.
- Mahapatra, D. K., Rao, A. D., Babu, S. V., & Srinivas, C. (2007). Influence of coast line on upper ocean's response to the tropical cyclone. *Geophysical Research Letters*, 34, L17603. <https://doi.org/10.1029/2007GL030410>.
- Maneesha, K., Murty, V. S. N., Ravichandran, M., Lee, T., Yu, W., & McPhaden, M. J. (2012). Upper ocean variability in the Bay of Bengal during the tropical cyclones Nargis and Laila. *Progress in Oceanography*, 106, 49–61. <https://doi.org/10.1016/j.pocean.2012.06.006>.
- Mei, W., Lien, C. C., Lin, I. I., & Xie, S. P. (2015). Tropical cyclone-induced ocean response: A comparative study of the South China Sea and tropical Northwest Pacific. *Journal of Climate*, 28, 5952–5968. <https://doi.org/10.1175/JCLI-D-14-00651.1>.
- Mei, W., Pasquero, C., & Primeau, F. (2012). The effect of translation speed upon the intensity of tropical cyclones over the tropical ocean. *Geophysical Research Letters*, 39, L07801. <https://doi.org/10.1029/2011GL050765>.
- Mrvaljevic, R. K., Black, P. G., Centurioni, L. R., Chang, Y.-T., D'Asaro, E. A., Jayne, S. R., Lee, C. M., Lien, R.-C., Lin, I.-I., Morzel, J., Niiler, P. P., Rainville, L., Sanford, T. B. (2013). Observations of the cold wake of Typhoon Fanapi (2010). *Geophysical Research Letters*, 40, 316–321. <https://doi.org/10.1029/2012GL054282>.
- Perrie, W., Ren, X., Zhang, W., & Long, Z. (2004). Simulation of extratropical Hurricane Gustav using a coupled atmosphere–ocean–sea spray model. *Geophysical Research Letters*, 31, L03110. <https://doi.org/10.1029/2003GL018571>.
- Price, J. F. (1981). Upper ocean response to a hurricane. *Journal of Physical Oceanography*, 11, 153–175. [https://doi.org/10.1175/1520-0485\(1981\)011<0153:UORTAH>2.0.CO;2](https://doi.org/10.1175/1520-0485(1981)011<0153:UORTAH>2.0.CO;2).
- Rao, R. R., & Sivakumar, R. (2003). Seasonal variability of sea surface salinity and salt budget of the mixed layer of the north Indian Ocean. *Journal Geophysical Research*, 108, C13009.
- Sengupta, D., Goddalahundi, B. R., & Anitha, D. S. (2008). Cyclone-induced mixing does not cool SST in the post-monsoon North Bay of Bengal. *Atmospheric Science Letters*, 9, 1–6. <https://doi.org/10.1002/asl.162>.
- Shang, S., Li, L., Sun, F., Wu, J., Hu, C., Chen, D., Ning, X., Qiu, Y., Zhang, C., Shang, S. (2008). Changes of temperature and bio-optical properties in the South China Sea in response to Typhoon Lingling, 2001. *Geophysical Research Letters*, 35, L10602. <https://doi.org/10.1029/2008GL033502>.
- Shi, W., & Wang, M. (2008). Three-dimensional observations from MODIS and CALIPSO for ocean responses to cyclone Nargis in the Gulf of Martaban. *Geophysical Research Letters*, 35, L21603. <https://doi.org/10.1029/2008GL035279>.
- Subrahmanyam, B., Rao, K. H., Srinivasa Rao, N., Murty, V. S. N., & Sharp, R. J. (2002). Influence of a tropical cyclone on Chlorophyll-*a* concentration in the Arabian Sea. *Geophysical Research Letters*, 29(22), 2065. <https://doi.org/10.1029/2002GL015892>.
- Sun, L., Yang, Y. J., Xian, T., Lu, Z., & Fu, Y. F. (2010). Strong enhancement of chlorophyll *a* concentration by a weak typhoon. *Marine Ecology Progress Series*, 404, 39–50. <https://doi.org/10.3354/meps08477>.
- Thadathil, P., Gopalakrishna, V. V., Muraleedharan, P. M., Reddy, G. V., Araligidad, N., & Shenoy, S. (2002). Surface layer temperature inversion in the Bay of Bengal. *Deep Sea Research Part I*, 49(10), 1801–1818. [https://doi.org/10.1016/S09670637\(02\)00044-4](https://doi.org/10.1016/S09670637(02)00044-4).
- Venkatesan, R., Mathew, S., Vimala, J., Latha, G., Muthiah, M. A., Ramasundaram, S., Sundar, R., Lavanya, R., Atmanand, M. A. (2014). Signatures of very severe cyclonic storm Phailin meteorological parameters observed by moored buoy network in the Bay of Bengal. *Current Science*, 107(4), 588–595.
- Vissa, N. K., Satyanarayana, A. N. V., & Prasad, K. B. (2012). Response of Upper Ocean during passage of MALA cyclone utilizing ARGO data. *International Journal of Applied Earth Observation and Geoinformation*, 14, 149–159.
- Vissa, N. K., Satyanarayana, A. N. V., & Prasad, K. B. (2013). Response of upper ocean and impact of barrier layer on Sidr cyclone induced sea surface cooling. *Ocean Science Journal*, 48, 279–288.
- Walker, N. D., Leben, R. R., & Balasubramanian, S. (2005). Hurricane-forced upwelling and chlorophyll *a* enhancement within cold-core cyclones in the Gulf of Mexico. *Geophysical Research Letters*, 32, L18610. <https://doi.org/10.1029/2005GL023716>.
- Wang, X. D., Han, G. J., Qi, Y. Q., & Li, W. (2011). Impact of barrier layer on typhoon-induced sea surface cooling. *Dynamics of Atmospheres and Oceans*, 52, 367–385. <https://doi.org/10.1016/j.dynatmoce.2011.05.002>.